ELSEVIER

Polymer 42 (2001) 4791–4802

polymer

www.elsevier.nl/locate/polymer

The radical homopolymerization of *N*-phenylmaleimide, *N*-*n*-hexylmaleimide and *N*-cyclohexylmaleimide in tetrahydrofuran

D.J.T. Hill[a,*], L.Y. Shao[a], P.J. Pomery[a], A.K. Whittaker[b]

[a]*Chemistry Department, Polymer Materials & Radiation Group and Centre for Magnetic Resonance, University of Queensland, St Lucia, Brisbane, Queensland 4072, Australia*

[b]*Centre for Magnetic Resonance, University of Queensland, St Lucia, Brisbane, Queensland 4072, Australia*

Received 2 July 2000; received in revised form 12 November 2000; accepted 26 November 2000

Abstract

The kinetics and mechanisms of thermally initiated (using 2,2′-azobisisoburyronitrile (AIBN) as initiator) radical homopolymerizations of a series of maleimides, including *N*-phenymaleimide (PHMI) [1-phenyl-1*H*-pyrrole-2,5-dione]; *N*-*n*-hexylmaleimide (*n*HMI) [1-(*n*-hexyl)-1*H*-pyrrole-2,5-dione]; and *N*-cyclohexylmaleimide (CHMI) [1-cyclohexyl-1*H*-pyrrole-2,5-dione] have been investigated in THF solution by an on-line FT-NIR technique. It was found that the order of the activation energies for the three *N*-sub-MIs is: $E_{a\ PHMI} < E_{a\ nHMI} < E_{a\ CHMI}$. The overall polymerization rate parameter k and the pre-exponential factor A were calculated. The kinetic order with respect to the *N*-sub-MIs was in the range of $0.71 < m < 0.75$ for the initiator and $n = 1.0$ for the monomer. Radical transfer to solvent was found to be the key factor in determining the apparent order with respect to the initiator.

All of the homopolymers had a relatively low molecular weight. The end groups of the polymer chains were characterized by MALDI-TOF, GPC and NMR methods and the results clearly indicate that the polymerization was initiated by THF radicals, and that the termination reaction is mainly controlled by chain transfer to solvent through an hydrogen abstraction mechanism.

Keywords: Maleimide; Free radical polymerization; Kinetics

1. Introduction

Many studies have been carried out on the free radical homopolymerization of *N*-sub-MIs. The focus has always been on the effect of the *N*-substituent on the reactivity of the monomer and/or the final physical and chemical properties of the polymer [1–10]. The rate of polymerization has been found to be influenced by solvent [7,11–14], initiator [8,13,15], temperature [8,13,16] and additives [5]. A literature review has outlined these influences on the homopolymerization of PHMI, *n*HMI, CHMI and other *N*-substituted maleimides [17,18].

However, the reason why the *N*-sub-MIs polymerization rates vary for different *N*-substituents is not clear. In addition, little work has been reported on the kinetics of the homopolymerization of MIs to high conversions, which is a necessary requirement for any practical application of these materials. Furthermore, the published kinetic parameters often vary significantly, even though in some cases the techniques used to obtain these data are the same.

Many modern instrumental techniques have been utilized to obtain kinetic rate parameters with a higher precision. Real time IR is one of the most useful methods [19–22]. However, in the mid-IR range, complicated peak fitting or deconvolution to overcome the significant peak overlapping problems usually is required [23]. In particular, in situ solution polymerization is very hard to follow by mid-IR because of the limitations of KBr windows. Therefore, near-IR (NIR) spectroscopy offers promising advantages for obtaining kinetic data because Pyrex cells of long path length may be used.

In the NIR region, the strongest absorption bands arise from overtones and combinations of the fundamental vibrations of =C–H, C–H, O–H and N–H [24]. These groups have significant molar absorptivities for these overtones because of the large anharmonicity of the vibrations which involve a light hydrogen atom and a heavier atom such as C, O, or N. In the NIR region, C–C, C=C, C=O, C–N bonds exhibit only very weak absorption bands, and the intensity of the C=C–H, O–H and N–H bands are 10 to 100 times weaker than in the mid-IR region. So, the NIR spectra are simpler than the mid-IR spectra with less band overlap, and through spectral accumulation, high quality spectra with

* Corresponding author. Tel.: +61-7-3365-4100; fax: +61-7-3365-3833.
E-mail address: hill@chemistry.uq.edu.au (D.J.T. Hill).

0032-3861/01/$ - see front matter
PII: S0032-3861(00)00867-3

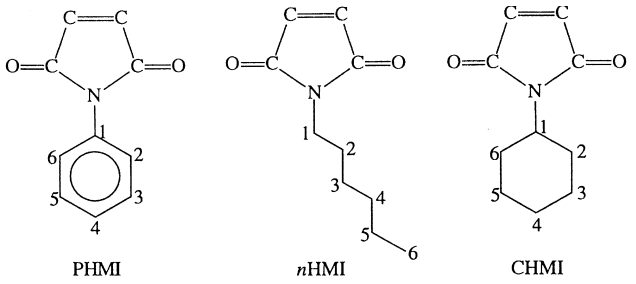

Fig. 1. The structure of PHMI, *n*HMI and CHMI.

excellent signal to noise can be obtained. Thus, in the NIR spectra the absorption bands for C=C–H, O–H, and N–H vibrations can be detected at levels as low as 0.0005 absorbance units [25], with an accuracy and precision equivalent to ultraviolet/visible (UV/Vis) spectroscopy. The detection limits are in the order of 0.1% [26].

In addition, the low molar extinction coefficients of these absorption bands make it easier to obtain linear Beer's Law relationships at higher concentrations. Despite the fact that only carbon tetrachloride and carbon disulfide are transparent throughout the entire NIR region, subtraction of the solvent background is facile and the use of conventional solution concentrations is acceptable [27]. Furthermore, as quartz or normal glassware can be used as the sample cell, the real benefit of working in the NIR region is the ability to measure samples in real time without special sample or cell (window) preparation.

In this study, three *N*-substituents (*N*-phenyl, *N*-*n*-hexyl, and *N*-cyclohexyl) were chosen to represent aromatic, aliphatic, and cyclic alkyl substituents, respectively (Fig. 1). AIBN has been used as the initiator. The polymerization experiments have been carried out in THF because: (a) it is a polar solvent in which all of the selected *N*-sub-MIs have the best solubility; (b) solution polymerization will reduce gelation interference; (c) the lack of literature data for polymerizations in THF.

The aim of this study was to investigate the kinetics and mechanism of the free radical solution homopolymerizations of PHMI, *n*HMI and CHMI. The results of the study should reveal the effect of the *N*-substituents and the solvent THF on the kinetics and mechanisms of the polymerizations. A new method for deriving the polymerization parameters by an on-line FT-NIR technique has been utilized, and a combination the techniques of NMR/GPC/MALDI-TOF MS has also been applied for characterization of the polymers.

2. Experimental

Syntheses of PHMI, *n*HMI and CHMI were carried out according to literature methods [28] with little modification. The relevant intermediates and crude monomers were recrystallized several times in petroleum spirit or ethanol before the desired purity was obtained. For CHMI, repeated sublimation was found to be the best and most efficient method for purification of the final product. AIBN was purified by recrystallizing twice from methanol. All *N*-sub-MIs and AIBN crystals were stored in dark containers and kept in a refrigerator before use. THF was refluxed with sodium chips under N_2 until dry and freshly distilled before use. The monomer purity was confirmed using FTIR, ^{13}C and ^{1}H NMR, and microanalysis and the data compared with literature values where available [18].

The polymerization mixtures were prepared in volumetric flasks using AIBN as the thermal initiator. Some experiments were also conducted in the absence of added initiator. However, no evidence for self-initiation was found for *n*HMI or CHMI, but PHMI did show evidence of a very slow polymerization in the absence of added initiator. The self-initiation of PHMI is discussed herein. After preparation, aliquots of the reaction mixtures were transferred into glass tubes (with i.d. ≈ 3.4 mm), and the samples were subjected to four freeze–thaw–degas cycles to remove the O_2, and then sealed under vacuum at a pressure of 4.0×10^{-2} Pa. The sealed sample tubes were immediately inserted into liquid N_2 to ensure no reaction before use. These operations were carried out in a dark room to prevent any premature photo initiation of polymerization.

Polymerization was facilitated by placing the sample tube in a thermal-controlled heating block at a predetermined temperature (± 0.5°C). The FT-NIR spectra were obtained using a Perkin–Elmer 1600 IR spectrometer. A computer program was used to acquire spectra over the range 6500–4500 cm^{-1} (usually coaddition of 32 scans) at 1–2 min intervals to high conversion.

Matrix-assisted laser desorption/ionization-time of flight mass spectrometry (MALDI-TOF MS), NMR and GPC measurements were conducted for identification of the polymer end group, repeating unit, and molecular weight. The MALDI-TOF mass spectra were obtained on a Micromass TOF-Spec E spectrometer in reflection mode using a 20 kV accelerating voltage with desorption using a N_2 laser. Mass spectra were generated by summing the results of 200 laser pulses. Quantitative NMR spectra were obtained in $CDCl_3$ solutions at 50°C using either a Bruker Advance DRX 500 or a Bruker AMX 400 (DEPT studies) instrument with a relaxation decay of 10 s and inverse-gated decoupling to suppress NOE effects. GPC measurements were made using a Waters 2690 instrument fitted with two linear μ-styragel columns at 50°C and RI, UV and Viscotek detectors. THF was used as the eluent (0.5 ml/min) and the instrument calibrations were made using low molar mass polystyrene standards.

3. Results and discussion

All of the *N*-sub-MIs have C=CH overtone peaks at about 6100 cm^{-1} (PHMI, 6098 cm^{-1}; *n*HMI, 6095 cm^{-1} and

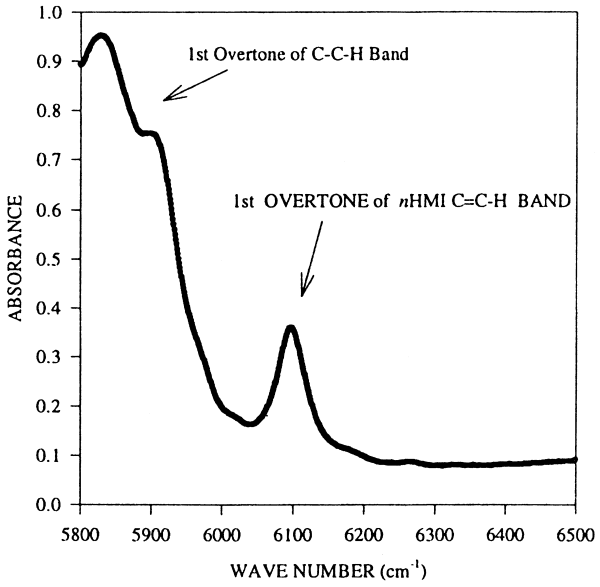

Fig. 2. *n*HMI FT-NIR spectrum, [*n*HMI] = 1.6 M, [AIBN] = 0.02 M, in THF, 60°C.

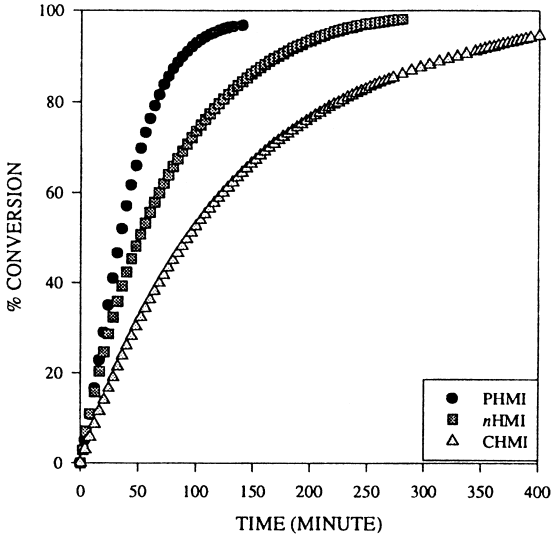

Fig. 4. Conversion–time profiles of solution homopolymerization of *N*-substituted maleimides, [MI] = 0.8 M, [AIBN] = 0.02 M, 60°C in THF.

CHMI, 6093 cm^{-1}). Fig. 2 gives the *n*HMI absorption spectrum over the range of 5800–6500 cm^{-1}. It is clearly shown that the C=CH peak of *n*HMI is well separated from the first overtone of the C=CH peak that is at about 5900 cm^{-1}. Beer–Lambert's law was shown to be valid for this vinyl band under the experimental conditions [18].

Since the peak area is directly proportional to the monomer concentration, the conversion–time profile can be easily derived from the spectra. Fig. 3 shows a three-dimensional plot for the *n*HMI C=CH overtone peak area–time profile. Similar 3D profiles were also obtained for the polymerization of PHMI and CHMI.

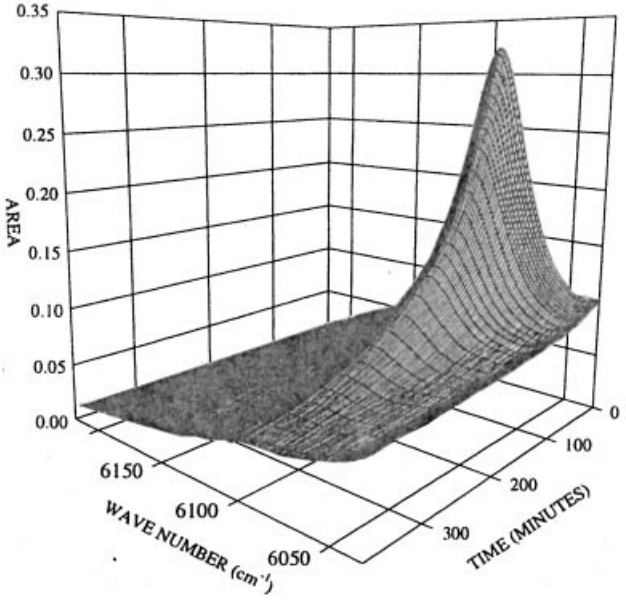

Fig. 3. In situ FT-NIR profile for *n*HMI homopolymerization, [*n*HMI] = 1.6 M, [AIBN] = 0.02 M, in THF, 60°C.

Fig. 4 shows a comparison of the conversion–time profiles for PHMI, *n*HMI and CHMI polymerizations at 60°C, [M] = 0.8 M, [I] = 0.02 M. The polymerization rates are in the order of PHMI > *n*HMI > CHMI under these conditions.

The polymerization rate (R_p) has been obtained by differentiation over the whole range of the conversion–time profile. In Fig. 5A, the conversion–time profiles for *n*HMI are shown for polymerizations over a range of initiator concentrations, and for a fixed initial *n*HMI concentration of 0.8 M. The corresponding rate curves in Fig. 5B have been derived from those in Fig. 5A by differentiation to yield the conversion dependence of the polymerization rate, which is seen to be dependent on the initial concentration of the initiator and also on the conversion. As the polymerization proceeds the monomer concentration decreases and so does R_p. This dependency can be described by Eq. (1).

$$R_p = k[I]^m[M]^n \quad (1)$$

where I is the initiator, *m* and *n* are the orders of the reaction with respect to I and M, respectively, and *k* is the overall polymerization rate constant, which obeys the Arrhenius equation.

Fig. 6A shows the conversion–time profile of *n*HMI at different initial monomer concentrations, and Fig. 6B shows the corresponding R_p versus conversion profile.

The initial rates of polymerization can be obtained from plots of the variation in the monomer concentration versus time. Fig. 7 shows the initial polymerization rates derived using this approach for the three *N*-sub-MIs for different initiator concentrations.

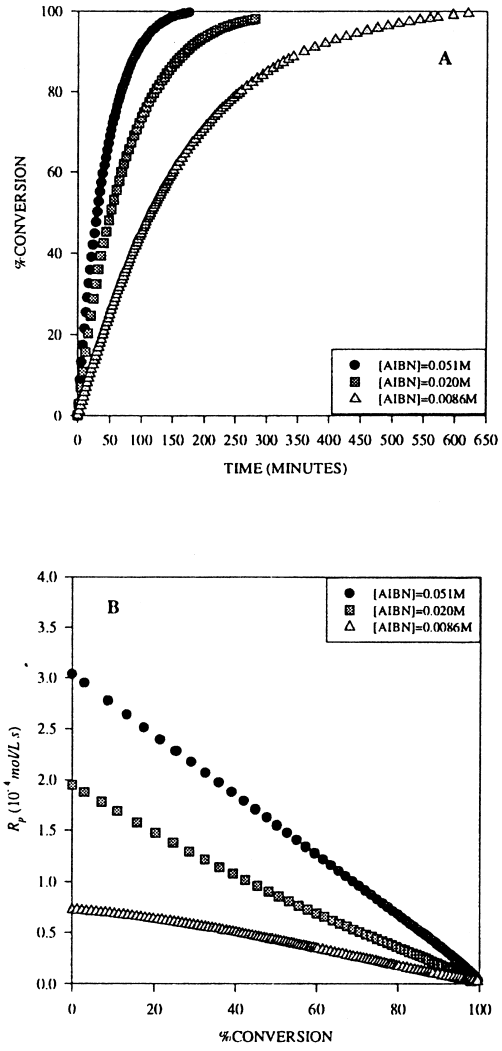

Fig. 5. (A) Conversion–time profiles for *n*HMI polymerization at variable initiator concentration and fixed [*n*HMI] = 0.8 M, 60°C in THF. (B) R_p–conversion profiles derived from (A).

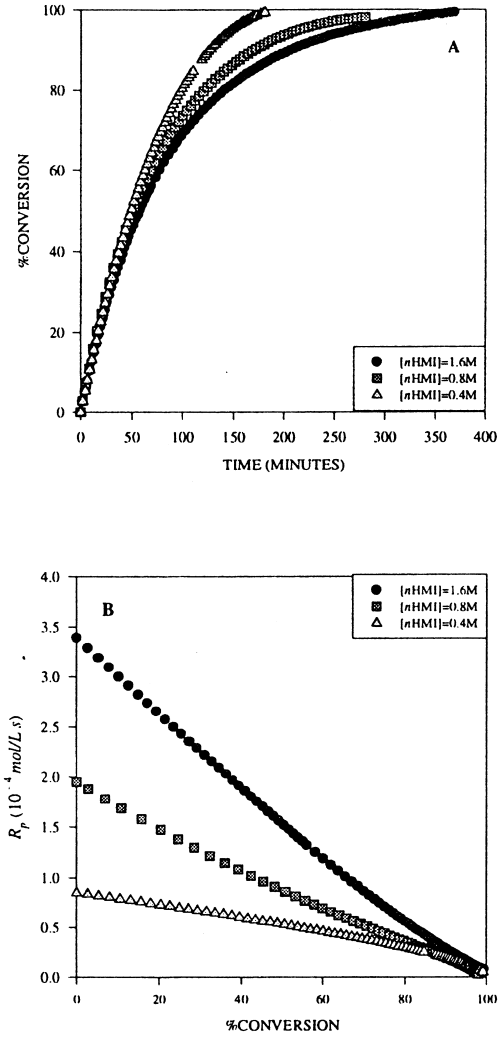

Fig. 6. (A) Conversion–time profiles for *n*HMI polymerization at variable monomer concentrations and fixed [AIBN] = 0.02 M, 60°C in THF. (B) R_p–conversion profiles derived from (A).

3.1. Determination of apparent initiator order (*m*)

In this study, the initial rates of polymerization (R_p) have been determined from the slope of the plot of monomer concentration [MI] versus time in the initial stages of the polymerization, as described above. Based on the values of the polymerization rates obtained from the plots in Fig. 7A–C, the relationship between $\log(R_p)$ and log[AIBN] will yield the order of the polymerization (*m*) with respect to the initiator Fig. 8.

3.2. Determination of apparent monomer order (*n*)

The reaction order for the monomer (*n*) can be determined using the same method as that used above for the initiator from data such as that in Fig. 9A for *n*HMI. In this case the initiator concentration was fixed while the monomer concentration was varied. From the slope of a plot of $\log(R_p)$ versus log[*n*HMI] (see Fig. 9B) a value of $n = 1.00$ for *n*HMI is obtained.

Alternatively, a plot of $\ln(R_p)$ versus ln[MI] for a fixed

Table 1
The kinetic parameters for PHMI, *n*HMI and CHMI homopolymerizations

Monomer	*m*	*n*	*k* (60°C) ($\text{mol}^{1-n-m}\,\text{l}^{m+n-1}\,\text{s}^{-1}$)	E_a (kJ/mol)	*A* ($\text{mol}^{1-n-m}\,\text{l}^{m+n-1}\,\text{s}^{-1}$)
PHMI	0.71 ± 0.02	1.00 ± 0.03	$(4.1 \pm 0.3) \times 10^{-3}$	90 ± 2	$(4.8 \pm 0.3) \times 10^{11}$
*n*HMI	0.75 ± 0.02	1.00 ± 0.03	$(3.0 \pm 0.2) \times 10^{-3}$	94 ± 2	$(1.9 \pm 0.2) \times 10^{12}$
CHMI	0.76 ± 0.02	1.00 ± 0.03	$(1.5 \pm 0.2) \times 10^{-3}$	102 ± 3	$(1.9 \pm 0.2) \times 10^{13}$

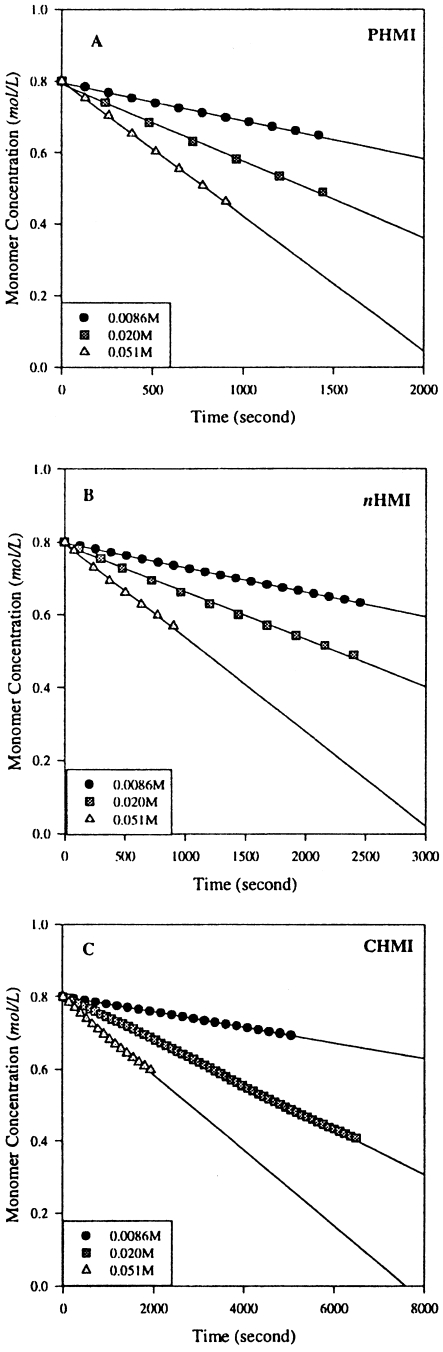

Fig. 7. Monomer concentration–time profiles for *N*-sub-MI homopolymerizations at a fixed initial monomer concentration ([MI] = 0.8 M) while varying AIBN concentrations (60°C in THF).

initiator concentration can be used to derive the value of *n* for each monomer. Fig. 10 shows that when the concentration of AIBN is fixed at 0.02 M and the initial monomer concentration is 0.8 M for each monomer a value of $n = 1.00$ is obtained.

3.3. Determination of the kinetic rate parameters

The R_p values at different temperatures for each monomer

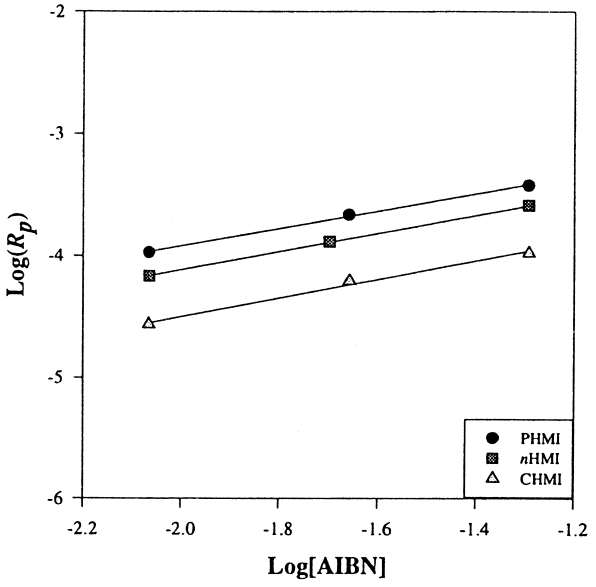

Fig. 8. Log(R_p) versus log[AIBN] plots for *N*-sub-MIs homopolymerization at fixed MI concentration ([MI] = 0.8 M) while varying AIBN concentration (60°C in THF).

have been derived from Fig. 11A–C. Based on the values for R_p, *m* and *n*, the overall polymerization rate parameter *k* can be calculated for polymerization at each temperature. Then from plots of ln*k* versus 1/*T* (Fig. 12), the pre-exponential factor, *A*, and the activation energy, E_a can be calculated (Eq. (2)). The values are presented in Table 1 together with the calculated values of *m* and *n*.

$$k = A\,\mathrm{e}^{-E_a/RT} \tag{2}$$

The relative values for activation energies for the three *N*-sub-MIs are in the order: $E_{a\ \mathrm{PHMI}} < E_{a\ n\mathrm{HMI}} < E_{a\ \mathrm{CHMI}}$. This variation in E_a can be explained by factors such as conjugation, steric and polar effects arising from the differences in the nature of the *N*-substituents.

3.4. The mechanism of polymerization

In a free radical polymerization,

$$-\frac{\mathrm{d[M]}}{\mathrm{d}t} = k_p\left(\frac{k_d f}{k_t}\right)^{1/2}[\mathrm{I}]^{1/2}[\mathrm{M}] = k[\mathrm{I}]^{1/2}[\mathrm{M}] \qquad \left(k = k_p\left(\frac{k_d f}{k_t}\right)^{1/2}\right) \tag{3}$$

Eq. (3) applies for termination dominated by polymer radicals under steady state conditions, $\mathrm{d[R^{\cdot}]}/\mathrm{d}t = 0$, which normally applies in inert solutions and in the early stages of bulk polymerizations. Eq. (3) is a special case of Eq. (1) with $m = 0.5$ and $n = 1$, which assumes that the reactivities of both the radical and the monomer are not modified by the solvent [29].

Modification of Eq. (3) is required especially when the polymerizations are carried out in solution where chain

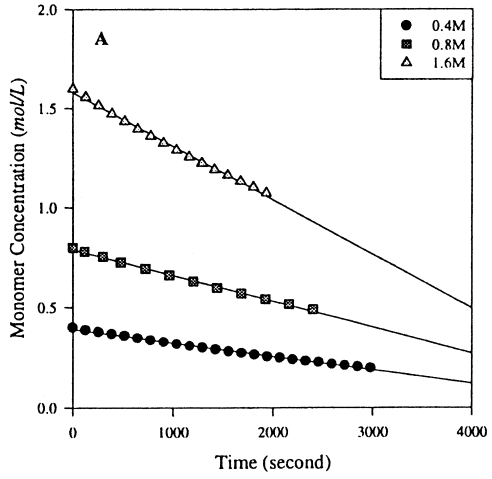

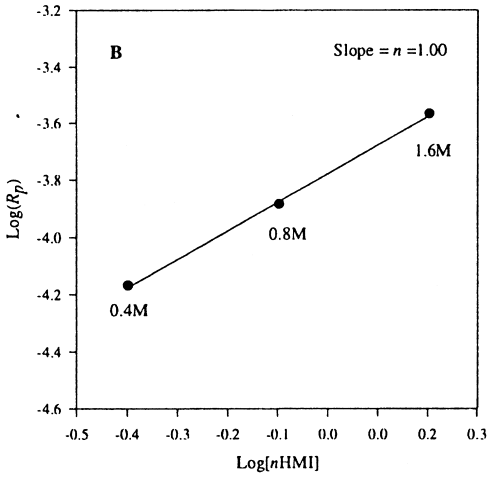

Fig. 9. Kinetic plots of *n*HMI homopolymerizations. (A) Monomer concentration versus time profiles at a fixed AIBN concentration ([AIBN] = 0.02 M) while varying monomer concentration (60°C in THF). (B) Log(R_p) versus log[M].

transfer reactions occur, which can be predominant in the polymerization.

If R$^{\cdot}$ represents any type of radical, which can include the initiator radical, I$^{\cdot}$, or propagating chain radical, P$^{\cdot}$, several possible types of transfer can take place:

1. To monomer

$$\left\{\begin{matrix}\mathrm{I}^{\cdot}\\ \text{or}\\ \mathrm{P}^{\cdot}\end{matrix}\right\} + \mathrm{M} \xrightarrow{k_{\mathrm{tr,M}}} \mathrm{M}^{\cdot} + \left\{\begin{matrix}\mathrm{I}\\ \text{or}\\ \mathrm{P}\end{matrix}\right\} \tag{4}$$

$$-\frac{\mathrm{d[R^{\cdot}]}}{\mathrm{d}t} = k_{\mathrm{tr,M}}[\mathrm{R}^{\cdot}][\mathrm{M}] \tag{5}$$

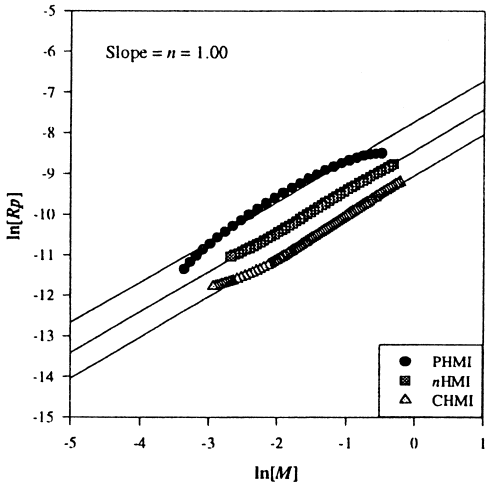

Fig. 10. ln R_p versus ln[MI] plots for *N*-sub-MIs homopolymerization (60°C in THF).

2. To solvent

$$\left\{\begin{matrix}\mathrm{I}^{\cdot}\\ \text{or}\\ \mathrm{P}^{\cdot}\end{matrix}\right\} + \mathrm{S} \xrightarrow{k_{\mathrm{tr,S}}} \mathrm{S}^{\cdot} + \left\{\begin{matrix}\mathrm{I}\\ \text{or}\\ \mathrm{P}\end{matrix}\right\} \tag{6}$$

$$-\frac{\mathrm{d[R^{\cdot}]}}{\mathrm{d}t} = k_{\mathrm{tr,S}}[\mathrm{R}^{\cdot}][\mathrm{S}] \tag{7}$$

For effective chain transfer to solvent the rate of polymerization is given by Eq. (3). So the order with respect to initiator (m) and monomer (n) under these circumstances are 0.5 and 1, respectively. If all solvent chain transfer radicals do not reinitiate polymerization, the relationship is more complex [30]. Depending on the extent to which the solvent radicals reinitiate polymerization, the order with respect to the initiator may vary between 0.5 and 1.0.

For degradative chain transfer to solvent, under a steady state concentration of radicals R$^{\cdot}$,

$$-\frac{\mathrm{d[M]}}{\mathrm{d}t} = k_{\mathrm{p}}\frac{2k_{\mathrm{d}}f[\mathrm{I}]}{k_{\mathrm{tr,S}}[\mathrm{S}] + k_{\mathrm{tr,M}}[\mathrm{M}]}[\mathrm{M}] = k_{\mathrm{p}}^{''}\frac{[\mathrm{I}][\mathrm{M}]}{k_{\mathrm{tr,S}}[\mathrm{S}] + k_{\mathrm{tr,M}}[\mathrm{M}]}$$

$$(k_{\mathrm{p}}^{''} = 2k_{\mathrm{p}}k_{\mathrm{d}}f) \tag{8}$$

Under these conditions the order for the monomer, n, would be observed to be less than one.

The order with respect to the initiator was found to be in the range of $0.71 < m < 0.76$ (± 0.02) for each *N*-sub-MI monomer. Many possible explanations for observation of an order of this magnitude have been proposed in the literature. For example, (1) both monomolecular and bimolecular termination occur simultaneously [31,32]; (2) the onset of a Trommsdorff effect [33] or heterogeneous polymerization [34]; (3) tautomerization of the monomer, which will

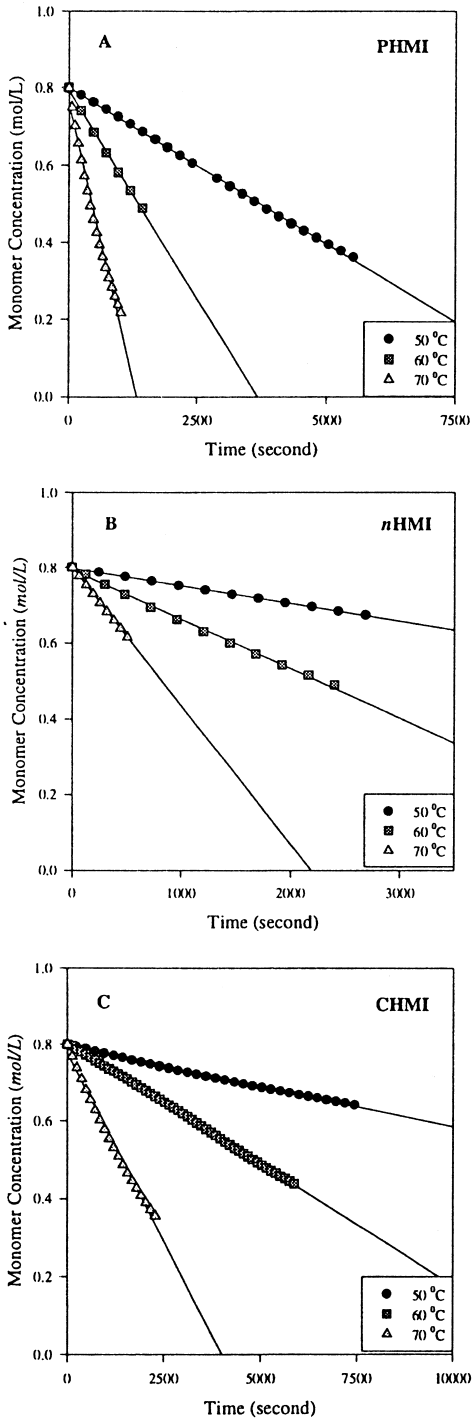

Fig. 11. Monomer concentration versus time profiles for *N*-sub-MI homopolymerization at different temperatures ([MI] = 0.8 M, [AIBN] = 0.02 M, 60°C, THF).

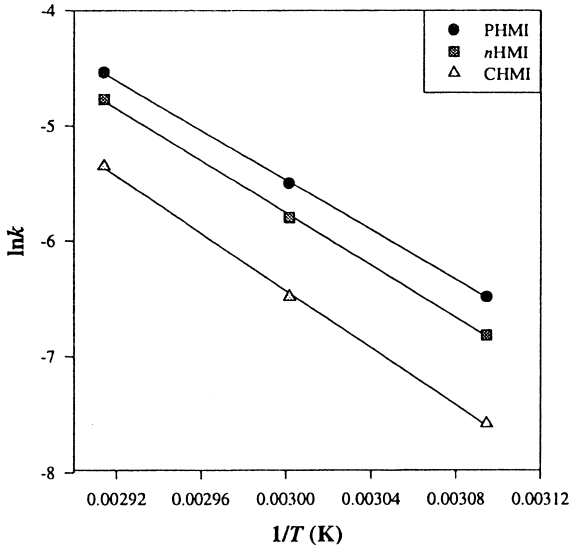

Fig. 12. ln *k* versus 1/*T* plots of *N*-sub-MI homopolymerizations ([MI] = 0.8 M, [AIBN] = 0.02 M, in THF).

introduce monomolecular termination [7]; (4) chain transfer to solvent or solvent retardation of polymerization [30,35].

For a bimolecular termination reaction the value of *m* should be 0.5, and if termination is monomolecular *m* should be 1. So, if both monomolecular and bimolecular termination occur simultaneously, the *m* values could be between 0.5 and 1. Monomolecular termination could occur at the wall of the polymerization vessel. If this occurs, the surface to volume ratio will influence the polymerization kinetics, but no such effect was observed. Gelation can also prompt monomolecular termination in systems with a high viscosity. While this may happen at high monomer concentration and/or in the high conversion range in this study, the calculations of the order of the initiator are based on low conversion data where gelation does not occur. A heterogeneous system would make the radical chain end more isolated, which may increase the probability of monomolecular termination. However, although poly-PHMI and poly-CHMI systems do become opalescent at high conversions, the poly-*n*HMI systems remain homogeneous throughout the whole conversion range. So heterogeneity, at least for the latter system, cannot be the cause for $m >$ 0.5. In addition, as the diketo tautomers of *N*-sub-MIs are among the most stable conformations in solution [36], termination via a tautomerization mechanism is unlikely.

The solvent retardation theory developed by Burnett and Loan [37] suggests that radicals of low reactivity can be produced by transfer to solvent, which can then react with monomer to reinitiate chains or they can become involved in termination reactions. In this situation, the kinetic chain length (and hence $\bar{M}_w$) will decrease [30] and *m* may become less than one. This is considered to be the explanation of the observed order for the systems studied herein.

3.5. NMR analyses of the polymer

In order to shed light on the termination mechanism an NMR analysis of the polymer was undertaken. The quatitative ^{13}C NMR spectra (see Fig. 13) showed that THF is incorporated into the poly-MI chains. The assignments of the THF peaks are shown in Fig. 13b. Confirmation of the

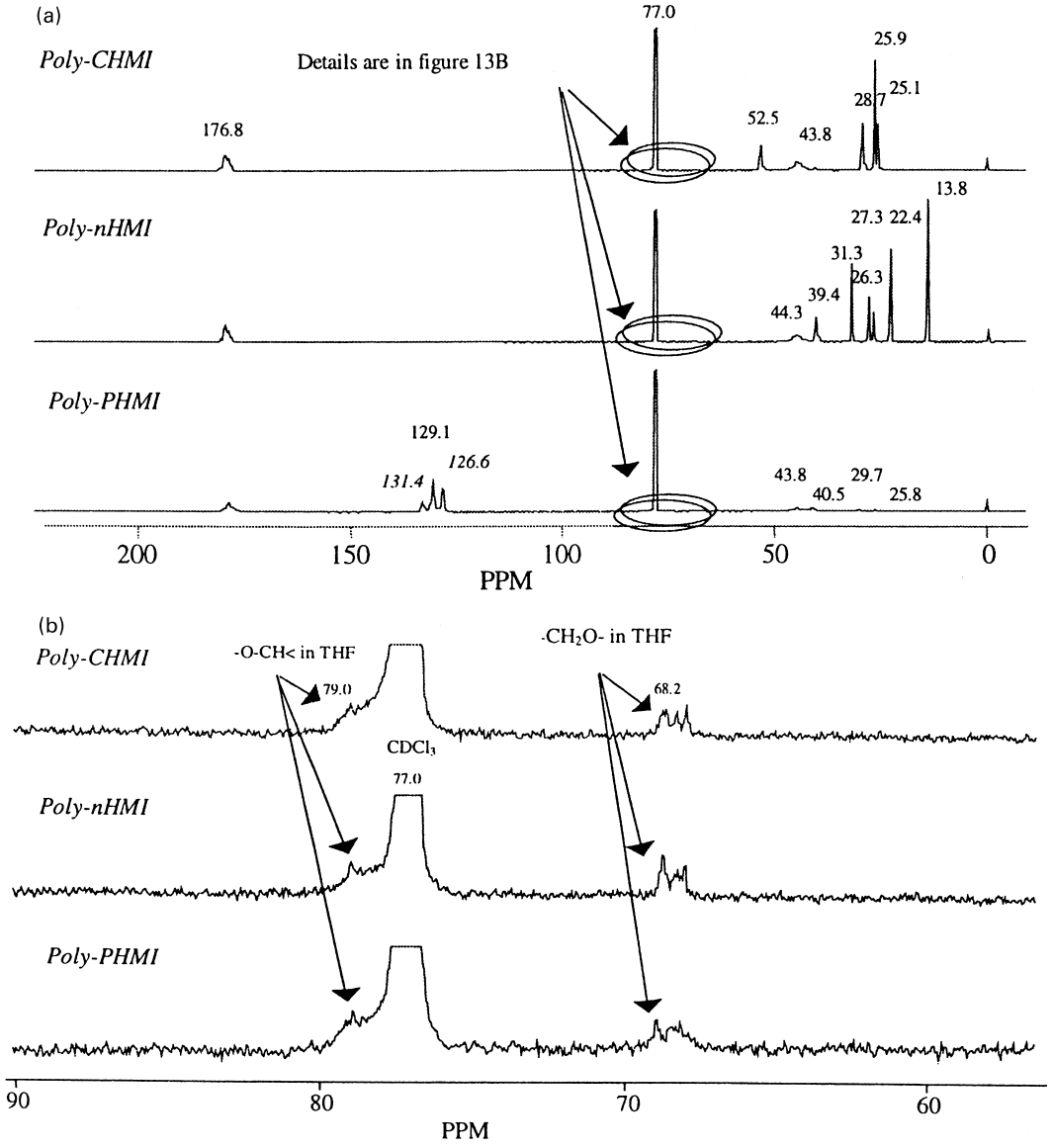

Fig. 13. (a) Quantitative ^{13}C NMR spectra for poly-*N*-sub-MIs (in $CDCl_3$, 50°C, inverse-gated decoupling to suppress NOE, relaxation delay: 10 s, NMR Bruker Avance DRX 500). (b) Peak assignment for THF chain ends peaks of THF by quantitative ^{13}C NMR (zoomed spectra from (a)).

peak assignment was made using an NMR DEPT 135 experiment (Fig. 14). The negative signal at $\delta = 68.2$ ppm (C_4, $-CH_2-O-$) and the positive signal at $\delta = 78.6$ ppm (C_1, $-O-CH<$) [38,39] in the DEPT 135 spectra clearly indicate that THF fragments are at the ends of the polymer chains.

In addition, no evidence for peaks from AIBN fragments, such as $-C^*H_3$, $-C^*(CN)(CH_3)_2$, $-C^*N$, which would be characterized by chemical shifts δ at about 14–22 and 120 ppm, was found in the NMR spectra. This indicates that AIBN does not directly participate in initiation of the polymerization. THF must therefore be involved in the initiation and/or termination steps of the polymerization. There is no evidence of any peaks in the NMR spectra of these poly-MIs which would be characteristic of C=C, which appear at about 134 ppm. This confirms that the principal chain termination reaction is not a bimolecular disproportionation.

Based on all the evidence outlined above, the following mechanism for the polymerization is proposed. On decomposition, the AIBN free radicals undergo transfer to THF according to reaction (6), and the resulting THF radical initiates the polymerization, becoming incorporated into the polymer chain. In the termination step, the polymer chain radical undergoes chain transfer to THF, so that the resulting polymer chains have a fragment of THF on one end and a proton on the other. The THF radicals formed upon termination can then either initiate a new chain or be

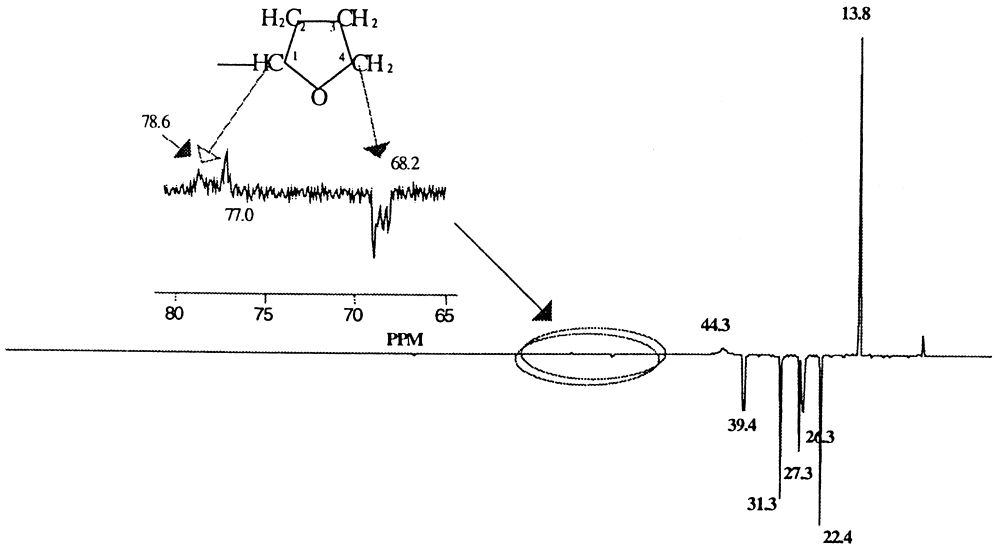

Fig. 14. Poly-*n*HMI DEPT 135 ^{13}C NMR spectrum, 30°C in $CDCl_3$ (NMR AMX400).

lost in a termination reaction, perhaps involving combination of two THF radicals, with a very small probability of a THF radical combining with a radical chain end producing a polymer chain with a fragment THF on both chain ends.

The NMR results and assumptions with respect to the polymerization mechanism are supported by previous ESR investigations [11]. In these studies of the UV initiated polymerizations of MIs, the *N*-alkyl-MI radical (I) and THF fragment radical (II) were found to coexist in a THF solution during polymerization (Fig. 15). It was postulated that an excited *N*-alkyl-MI can abstract a hydrogen atom from the solvent, such as THF, ethanol, or cyclic ethers. Radicals (I) or (II) can easily initiate the polymerization of the MI to produce the chain radical (III) or a THF ended radical (IV). In the case of termination by a combination of radicals (III) and (IV), a chain with a THF fragment on one end and proton on the other will be formed.

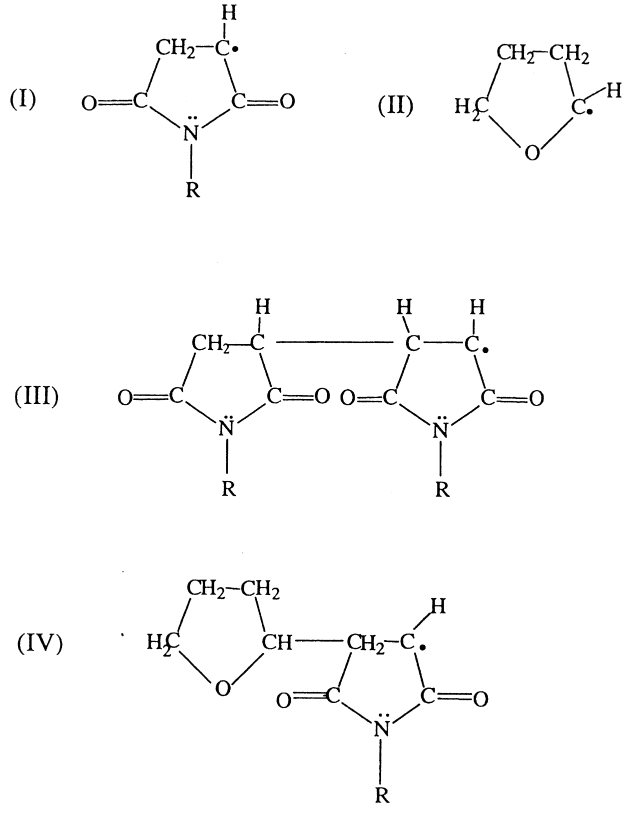

Fig. 15. Possible free radicals for *N*-sub-MI homopolymerization in THF, detected by ESR.

3.6. Molecular weight and end group analysis by MALDI-TOF, GPC and NMR

The MALDI-TOF mass spectrum of a poly-PHMI sample is shown in Fig. 16. All of the ions observed in the spectrum were molecular ions formed by attachment of a cation during the ionization process. Furthermore, all of the polymer species were singly-charged ions so that the mass to charge ratio, *m*/*z*, was equal to the mass of the ion.

In Fig. 16, a distribution of polymeric ions can be seen between *m*/*z* 790 and *m*/*z* 7377 with a maximum peak at *m*/*z* 2171. The peaks in this distribution are separated by intervals of *m*/*z* 173.17, which corresponds to the mass of the poly-PHMI repeat unit. The mass of the most intense peak, at *m*/*z* 2171.33, corresponds to the molecular ion of a poly-PHMI oligomer consisting of 12 units with a hydrogen atom at one end and a THF fragment at the other ($m = 71$), A sodium ion ($m = 23$) is associated with the oligomer in the mass measurement. The smaller satellite peaks (expanded in Fig. 16) at *m*/*z* 2149.24 and *m*/*z* 2187.26 are attributed to the attachment of a hydrogen and a potassium ion ($m = 39$), respectively. The masses of all of the peaks in the observed mass distribution correspond to molecular ions of poly-PHMI oligomers with chain lengths varying from 4 units at *m*/*z* 790, to 42 units at *m*/*z* 7377.

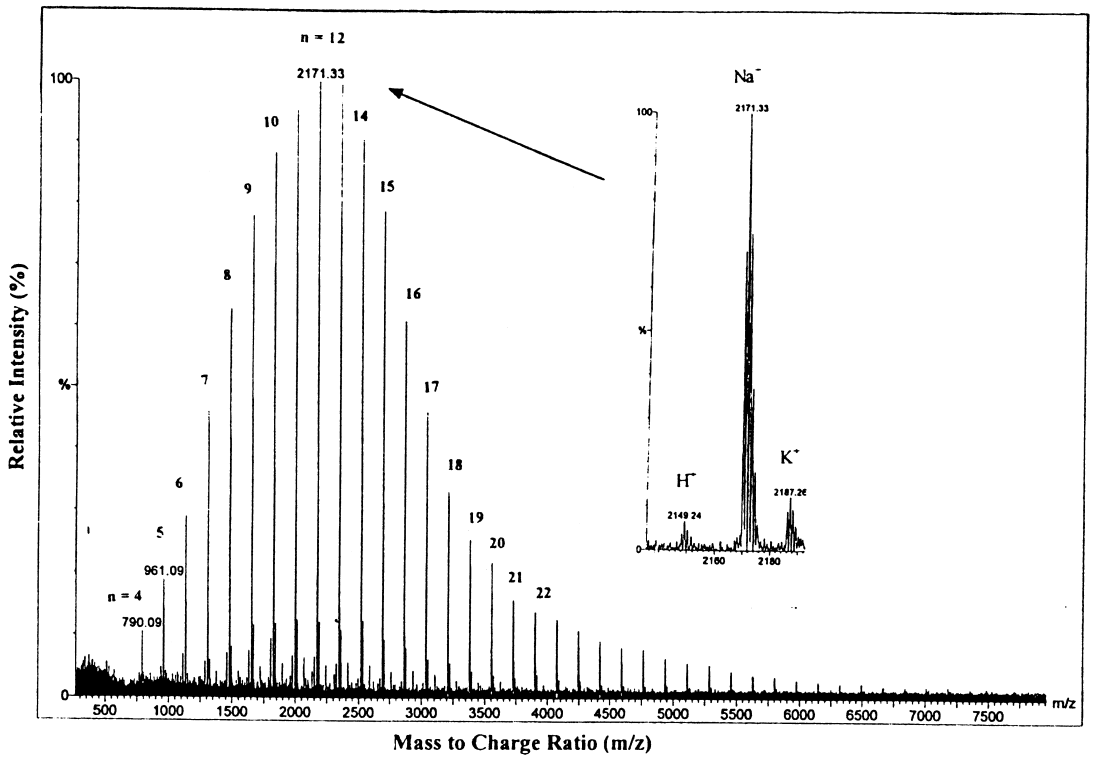

Fig. 16. MALDI-TOF MS spectrum of poly(*N*-phenylmaleimide).

The mass of the predominant end group of poly-MIs chains is equal to 72 and is independent of the length of the polymer chain. However, a small number of chains (<5%) were found to have a THF unit on both ends, which means that they are terminated either by combination of two chain propagation radicals or by combination of a propagation radical and a THF radical. The MALDI-TOF spectra of the poly-MIs also clearly confirmed that AIBN is not the species responsible for initiation of the polymerization of the MIs.

The quantitative NMR results can yield a value for ratio of the number of repeating units of *N*-sub-MIs to the THF fragment on the chain end (calculated from the peak intensity ratio of the C=O to that of the THF fragment $-CH_2-O-$ in Fig. 13). For *n*HMI/THF and CHMI/THF ratios of 16 ± 1 were obtained, while that for PHMI/THF was 13 ± 1. A GPC investigation for poly-*n*HMI yield an $\bar{M}_n$ of 2801 ± 147 g/mol, which corresponds to 15 ± 1 repeating *n*HMI units in each chain if the mass of the chain end unit (THF fragment + proton) is 72. So, both the NMR and GPC results agree with those obtained from MALDI-TOF. Close agreement was also obtained between the average $\bar{M}_n$ results from MALDI-TOF and those obtained from GPC and NMR analyses. A summary of the results obtained from the three methods (^{13}C NMR, GPC and MALDI-TOF) is shown in Table 2.

So the conclusion can be drawn that the nature of the *N*-substituents in the MIs do not affect the average number of units per chain, and the low molecular weight of the poly-MIs arises through chain transfer to solvent. Predominantly there is one THF per chain and the another chain end is terminated by proton, which provides experimental evidence for the mechanism of initiation and termination.

Table 2
^{13}C NMR, GPC and MALDI-TOF results for poly-PHMI, poly-*n*HMI and poly-CHMI

Polymer	Ratio of MIs/THF (^{13}C NMR)	$\overline{DP}_n$ (GPC/MALDI)	$\bar{M}_n$ (g/mol) (GPC/MALDI)	$\bar{M}_w$ (g/mol) (GPC)	PD (GPC)
PHMI	13 ± 1	16.6(M)	2942(M)	[a]	[a]
*n*HMI	16 ± 1	15 ± 1(G) 14.2(M)	2801 ± 147(G) 2637(M)	5526 ± 121	2.0 ± 0.1
CHMI	16 ± 1	14.9(M)	2743(M)	[a]	[a]

[a] The polymers were not completely soluble in the GPC solvent.

Table 3
The wavelength for maximum UV/Vis absorbance of PHMI, *n*HMI and CHMI in different solvents

Monomer	λ_{max} (nm)			
	Benzene	*n*-Hexane	THF	Ethanol
PHMI	320.0	320.0	314.6	312.7
*n*HMI	299.4	295.7	298.8	298.9
CHMI	303.0	299.2	300.3	300.6

3.7. Order with respect to monomer

The kinetic order for these *N*-sub-MI monomers has been found to be unity, which clearly indicates:

1. Chain transfer to monomer does not take place.
2. No termination occurs between growing polymer radicals and primary initiator radicals [33], which would yield an order of two with respect to the MI.

According to the model for polymerization expressed in Eq. (3) the order with respect to the monomer should be one. Thus the value of one obtained from the experimental data for the poly-MI systems agrees with the theoretical prediction.

3.8. Reactant–solvent complex (RSC) model

N-sub-MIs are strong electron acceptors and THF is an electron donor with two lone pair electrons. Thus, a donor–acceptor complex can be formed between the monomer and solvent, which may change the effective reactivity of *N*-sub-MI. It has been reported that in the solution polymerizations, radicals (both complexed and uncomplexed) may react faster with a complexed monomer than with uncomplexed monomer [40]. Moreover, it has been found in the present study that the PHMI is the only monomer among the three that could be 'self-initiated' in THF at 60°C. It is proposed that this behavior of PHMI is due to complex formation with the THF solvent.

A study of the UV/Vis spectra revealed a strong hypsochromic shift for PHMI for solutions in polar solvents as compared to nonpolar solvents, such as Bz or *n*-hexane. The hypsochromic shift was not observed for *n*HMI or CHMI under the same experimental conditions. These observations indicate that THF only affects the $n > \pi^*$ Franck–Condon excited state of PHMI carbonyl groups. The $n > \pi^*$ excited state of a carbonyl group is less dipolar than the ground state. During the process of excitation, one *n*-electron is promoted from a nonbonding orbital on the oxygen atom of the C=O group to an antibonding π^* orbital which is delocalized over the carbonyl group. Removal of an electron from the oxygen atom implies a considerable contribution by the $>\bar{C}-\bar{O}^{\oplus}$ mesomeric structure, with a decrease or even reversal in the direction of the excited-state dipole moment. This dipole diminution corresponds to a hypsochromic shift of the $n > \pi^*$ absorption band with increasing solvent polarity ($\nu(n > \pi^*)/\mathrm{cm}^{-1} \approx 31,000$) [41].

The reversal in the direction of the excited-state dipole moment allows the PHMI to form a strong RSC with the THF. This may explain why PHMI is the only monomer among the three that can be self-initiated, and why the PHMI polymerization is faster than that for the other two MIs. Table 3 shows the results of the UV/Vis investigation.

4. Conclusions

The kinetic orders of PHMI, *n*HMI and CHMI for polymerization are in the range of $0.71 < m < 0.75$ for the initiator and $n = 1.0$ for the monomer. Radical transfer to solvent was found to be the key factor in determining the order with respect to the initiator. The overall polymerization rate parameter k and the pre-exponential factor A have been calculated. The polymers formed in the reactions were found to have similar $\overline{DP}_n$, and there was no evidence for primary radical termination.

THF was found to be the chain end initiator fragment for all the MI polymers (PHMI, *n*HMI, CHMI), and there was no evidence for the presence of any AIBN fragments, which indicates that the AIBN radicals readily undergo chain transfer to THF. There was only one THF unit per chain with a proton at the other chain end. No evidence for C=C groups was found, which suggests that the termination is controlled by chain transfer to solvent. This also explains the low molecular weights of the polymers prepared in THF as solvent.

Solvation, complexation, and steric effects are believed to play a role in determining the polymerization rates through complexation with the solvent, which is particularly important for these systems.

The in situ FT-NIR method has proved to be a powerful tool for studies of polymerization kinetics. In combination with polymer molecular weight characterization by several independent techniques, such as MALDI-TOF, NMR and GPC, the mechanisms for polymerization of these *N*-sub-MIs in THF have been elucidated.

Acknowledgements

Special thanks to Dr Susan Hunt of the Queensland University of Technology, Australia, for her invaluable MALDI-TOF analysis, and to Miss Lynette Lambert of the University of Queensland, Australia, for assistance with the quantitative NMR analyses.

References

[1] Matsumoto A, Kubota T, Otsu T. Macromolecules 1990;23:4508–13.
[2] Otsu T, Matsumoto A, Kubota T, Mori S. Polym Bull 1990;23:43–50.
[3] Oishi T, Kimura T. Kobunsh Ron 1976;33:685–91.

[4] Oishi T, Fujimoto M. J Polym Sci, Polym Chem Ed 1984;22:2789–890.
[5] Sabee AZE, Mokhtar S. Eur Poylm J 1983;19:451–6.
[6] Oishi T, Yamasaki H, Fujimoto M. Polym J 1991;23:795–804.
[7] Lokaj J, Hrabak F. Eur Poylm J 1978;14:1039–43.
[8] Wang JJ, Chern YT, Chung MA. J Polym Sci, Part A: Polym Chem 1996;34:3345–54.
[9] Matsumoto A, Kimura T. J Macromol Sci, Pure Appl Chem 1996;A33:1049–61.
[10] Parker SF. Spectrochim Acta, Part A 1995;51:2067–72.
[11] Aida H, Takase I, Nozi T. Makromol Chem 1989;190:2821–31.
[12] Qiu K, Ye K. Acta Polym Sin 1993;1:125–8 (in Chinese).
[13] Matsumoto A, Kubota T, Ito H, Otsu T. Mem Fac Engng, vol. 31. Osaka City Univ, 1990. p. 47–59.
[14] Oishi T, Sase K, Saeki K, Yao S, Ohdan K. Polymer 1997;36:3935–42.
[15] Yamada M, Takase I, Koutou N. Polym Lett 1968;6:883–8.
[16] Iwatsuki S, Kubo M, Wakita M, Matsui Y, Kanoh H. Macromolecules 1991;24:5009–14.
[17] Shao LY. Maleimides in free radical polymerization, chap. 1: introduction. PhD thesis. The University of Queensland, Australia, 2000. p. 1–16.
[18] Shao LY. Maleimides in free radical polymerization, chap. 2: the homopolymerization of PHMI, *n*HMI and CHMI. PhD thesis. The University of Queensland, Australia, 2000. p. 17–54.
[19] Decker C, Moussa K. Macromolecules 1989;22:4455–62.
[20] Sheridan RE, Rein AJ. R & D Mag 1991;October:100–2.
[21] Decker C. In: Krongauz VV, Trifunac AD, editors. Processes in photoreactive polymers. New York: Chapman & Hall, 1995. p. 34–55.
[22] George GA, Cole-Clarke P, John NS, Friend G. J Appl Polym Sci 1991;42:643–57.
[23] Kleinová A, Borsig E, Schulze U, Pionteck J. Macromol Chem Phys 1996;197:2289–96.
[24] Skoog DA, Leary JJ. Principles of instrumental analysis. 4th ed. Sydney: Saunders, College Publishing, 1992 (p. 275–8).
[25] Rogers J. Testing technology. NSW, Australia: Stadvis Pty Ltd, 1996 (April/May, p. 34–5).
[26] Skoog DA, Leary JJ. Principles of instrumental analysis. 4th ed. Sydney: Saunders, College Publishing, 1992 (p. 285–7).
[27] Long TE, Liu HY, Schell BA, Teegarden DM. Polym Mater Sci Engng Prepr 1994;71:146–7.
[28] Searle NE (Inventor). Synthesis of *N*-aryl-maleimides. US patent, USA 2444536, 1948.
[29] Moad G, Solomon DH. The chemistry of free radical polymerization. New York: Pergamon, 1995 (vol. 1, p. 315–45).
[30] North AM, Postlethwaite D. In: Tsuruta T, O'Driscoll KF, editors. Structure and mechanism in vinyl polymerization. New York: Marcel Dekker, 1969. p. 99–124.
[31] Oishi T. Polym J 1980;12:719–27.
[32] Cowie JMG. In: Cowie JMG, editor. Alternating copolymers. New York: Plenum Press, 1985. p. 19–74.
[33] Odian GG. Principles of polymerization. New York: McGraw-Hill, 1970 (p. 175–255 and 262–5).
[34] Oishi T. Kobunsh Ron 1991;48:123–8.
[35] George MH. In: Ham GE, editor. Vinyl polymerization. New York: Marcel Dekker, 1967 (part 1, p. 158–63).
[36] Acker A, Hofmann HJ, Cimiraglia R. J Mol Struct (Theochem) 1994;121:43–51.
[37] Burnett GM, Loan LD. Trans Faraday Soc 1953;49:214–8.
[38] Johnson LF, Jankowski WC. Carbon-13 NMR spectra. New York: Wiley, 1972 (p. 123).
[39] Bruch MD, Dybowski C. In: Bruch MD, editor. NMR spectroscopy techniques, 2nd ed. New York: Marcel Dekker, 1996. p. 61–105.
[40] Czerwinski WK. Makromol Chem 1993;194:3015–29.
[41] Reichardt C. In: Reichardt C, editor. Solvents and solvent effects in organic chemistry, 2nd ed. New York: VCH, 1988.